JACS
JOURNAL OF THE AMERICAN CHEMICAL SOCIETY
Communication
pubs.acs.org/JACS

Excitation Wavelength Dependent O_2 Release from Copper(II)–Superoxide Compounds: Laser Flash-Photolysis Experiments and Theoretical Studies

Claudio Saracini,[†] Dimitrios G. Liakos,[‡] Jhon E. Zapata Rivera,[§] Frank Neese,[‡] Gerald J. Meyer,[†] and Kenneth D. Karlin*[,†]

[†]Department of Chemistry, The Johns Hopkins University, Baltimore, Maryland 21218, United States
[‡]Max-Plank-Institut für Chemische Energie Konversion, Stiftstrasse 34-36, 45470 Mülheim, Germany
[§]Departament de Quimica Fisica i Inorganica, Universitat Rovira i Virgili, c/Marcel·lí Domingo, s/n, 43007 Tarragona, Spain

Supporting Information

ABSTRACT: Irradiation of the copper(II)–superoxide synthetic complexes $[(TMG_3tren)Cu^{II}(O_2)]^+$ (**1**) and $[(PV\text{-}TMPA)Cu^{II}(O_2)]^+$ (**2**) with visible light resulted in direct photogeneration of O_2 gas at low temperature (from −40 °C to −70 °C for **1** and from −125 to −135 °C for **2**) in 2-methyltetrahydrofuran (MeTHF) solvent. The yield of O_2 release was wavelength dependent: λ_{exc} = 436 nm, ϕ = 0.29 (for **1**), ϕ = 0.11 (for **2**), and λ_{exc} = 683 nm, ϕ = 0.035 (for **1**), ϕ = 0.078 (for **2**), which was followed by fast O_2-recombination with $[(TMG_3tren)Cu^{I}]^+$ (**3**) and $[(PV\text{-}TMPA)Cu^{I}]^+$ (**4**). Enthalpic barriers for O_2 rebinding to the copper(I) center (~10 kJ mol^{-1}) and for O_2 dissociation from the superoxide compound **1** (45 kJ mol^{-1}) were determined. TD-DFT studies, carried out for **1**, support the experimental results confirming the dissociative character of the excited states formed upon blue- or red-light laser excitation.

Copper-containing proteins play a major role in O_2 transport and activation in biology. Thus, Cu^I/O_2 reactions and subsequent transformations are critical in this setting as well as in practical systems.[1] Initial O_2 adducts of copper(I) must form in all cases, including in O_2 carriers, oxygenases (oxygen transfer to the substrate), and oxidases (substrate oxidized by O_2), but these first-formed species often further react with other electron/proton sources (which may be the substrate) to give Cu_n/peroxo, Cu^{II}/hydroperoxo[2,3] or perhaps Cu_n/oxyl[1b,4] active species or intermediates. In peptidylglycine α-hydroxylating monooxygenase[5] and dopamine β-monooxygenase,[6] such O_2 activation occurs at a single copper center. An X-ray structure of a precatalytic complex along with chemical[7] and computational studies[4a,8] suggested an end-on bound Cu^{II}/superoxide species as the enzyme reactive intermediate effecting substrate hydrogen abstraction, further implicating the (bio)chemical importance of initially formed Cu^I/O_2 1:1 adducts, i.e., Cu^{II}/superoxide species.

Here, for the first time, we show that O_2 can be photoejected directly from the 1:1 mononuclear copper/O_2 compounds $[(TMG_3tren)Cu^{II}(O_2)]^+$ (**1**) and $[(PV\text{-}TMPA)Cu^{II}(O_2)]^+$ (**2**) using either 436 or 683 nm pulsed laser light (Scheme 1). Interestingly, a different yield for O_2 release was observed with these two excitation wavelengths which is different if compared to the O_2 photorelease found in heme systems such as myoglobin.[9] Temperature-dependent kinetic studies and thermodynamic studies have been carried out to elucidate the nature of the barriers and the stability of the species involved in the O_2 binding and dissociation processes. Data are corroborated by DFT calculations that help to (a) explain why O_2 photorelease is observed and (b) interpret the experimentally observed excitation wavelength-dependent quantum yield for the O_2 photorelease through new insights into the evolution of the excited states along the copper/oxygen reaction coordinate. To the best of our knowledge, this is the first time that a direct O_2 photoejection from 1:1 copper/superoxide adducts has been shown to occur.

Scheme 1

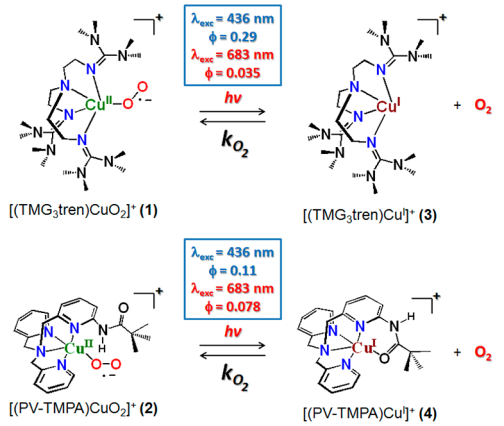

Oxygenation of **3** at low temperature in MeTHF was accompanied by a drastic color change of the solution, from colorless to green, forming the previously well-characterized compound **1**[10] and leading to the red spectrum shown in Figure 1A. Oxygenation of **4** at low temperature also yielded the previously characterized mononuclear copper/O_2 species **2** (see Supporting Information [SI] for UV–visible spectra).[11] Cleavage of the copper–oxygen bond was then induced upon

Received: November 17, 2013
Published: January 15, 2014

   dx.doi.org/10.1021/ja4115314 | J. Am. Chem. Soc. 2014, 136, 1260–1263

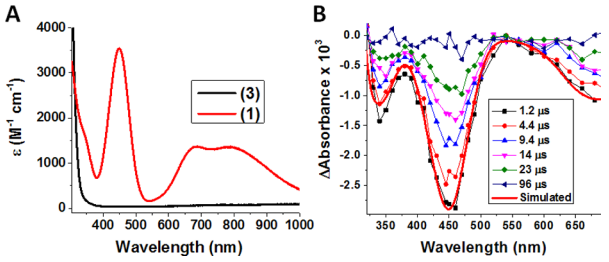

Figure 1. (A) Absorption spectrum of **1** (red line) obtained from oxygenation of **3** (black line) at 218 K in MeTHF. (B) Transient absorption difference spectra collected at the indicated delay times after 436 nm laser excitation (15 mJ/pulse, 8–10 ns fwhm) of **1** in MeTHF at 218 K. Overlaid in red on the experimental data is a simulated spectrum (Abs(**3**) − Abs(**1**)).

laser excitation of **1** and **2** (λ_{exc} = 436 or 683 nm) as shown by the transient absorption spectral data collected after laser excitation for **1**. These spectra were in complete agreement with that expected for O_2 photorelease from **1** to yield **3** (Figure 1B) and from **2** to yield **4** (see SI). The products of the reaction (**3**, O_2 and **4**, O_2, respectively) were excitation wavelength independent, although the quantum yields differed markedly: ϕ = 0.29 for **1** and ϕ = 0.11 for **2** (λ_{exc} = 436 nm), ϕ = 0.035 for **1** and ϕ = 0.078 for **2** (λ_{exc} = 683 nm). The appearance of the products, **3** and **4**, occurred within the instrument response time indicating an O_2 time release of less than 10 ns.

The follow-up thermal reaction of $[(TMG_3tren)Cu^I]^+$ (**3**) with O_2 led to the formation of the initial compound **1** as shown in Figure 1B. Kinetic parameters for O_2 coordination to **3** were quantified on the basis of microsecond time scale data. Thus, a plot of the observed rate constants versus the O_2 concentration under pseudo-first-order conditions (excess of O_2) revealed a linear correlation that allowed the determination of the second-order rate constants for O_2 coordinating to **3**, i.e., $k_{O_2} = 2.1 \times 10^6$ M^{-1} s^{-1} at −80 °C . For the same temperature, this compares to $k_{O_2} = 6.6 \times 10^5$ M^{-1} s^{-1} for **4** (Table 1).

The linear plots of k_{obs} vs $[O_2]$ had a positive intercept that was indicative of the presence of an equilibrium between the reacting species, O_2 and **3** (see SI). Such a positive intercept was not observed for the coordination of O_2 to **4** which indicated a quantitative formation of **2** from **4** and O_2. Consequently, rate constants for O_2 dissociation from **2** and equilibrium constants for the reaction between **4** and O_2 to give **2** could not be determined here. However, we were able to determine the equilibrium constant at several temperatures in MeTHF solvent through benchtop titration experiments for the binding of O_2 to **3**, to give **1** (Table 1 and SI). Equilibrium constant values were also determined from laser experiments as follows. In pseudo-first-order conditions, the rate law for O_2 binding to **3** is expressed by the equation $k_{obs} = k_{O_2}[O_2] + k_{-O_2}$ where k_{obs} is the observed rate constant, k_{O_2} is the second-order rate constant for the binding between **3** and O_2, and k_{-O_2} is the first-order rate constant for the dissociation reaction of O_2 from **1** (see section 6 of the SI). The values of k_{O_2} and k_{-O_2} were determined from laser experiments as a function of temperature through which the equilibrium constants were determined from the ratios k_{O_2}/k_{-O_2}. Van't Hoff analysis (see section 5 of the SI) of the equilibrium constants determined with the two different methods (titration experiments and laser experiments) led to

Table 1. Comparison of Kinetic and Thermodynamic Parameters for O_2 Binding and Dissociation for $[(L)Cu]^+$ Adducts

	k_{O_2}	k_{-O_2}	K_{O_2}
TMG_3tren^c			
$\Delta H^{\ddagger}$or ΔH^{0a}	10 ± 6	45 ± 7	−40 ± 2
$\Delta S^{\ddagger}$or ΔS^{0b}	−70 ± 26	42 ± 34	−134 ± 11
k or K 25 °C	(2.7 ± 1.2) × 10^7	(1.5 ± 0.8) × 10^7	∼1
k or K −80 °C	(2.1 ± 1.0) × 10^6	(5.2 ± 2.0) × 10^2	(6.3 ± 1.9) × 10^3
PV-TMPA^c			
	k_{O_2}	k_{-O_2}	K_{O_2}
$\Delta H^{\ddagger}$or ΔH^{0a}	9 ± 1	–	–
$\Delta S^{\ddagger}$or ΔS^{0b}	−97 ± 7	–	
k or K 25 °C	(4.8 ± 2.8) × 10^7	–	–
k or K −80 °C	(6.6 ± 3.5) × 10^5	–	–
TMPA^d			
	k_{O_2}	k_{-O_2}	K_{O_2}
$\Delta H^{\ddagger}$or ΔH^{0a}	7.62	58.0	−48.5
$\Delta S^{\ddagger}$or ΔS^{0b}	−45.1	105	−140
k or K 25 °C	1.3 × 10^9	1.3 × 10^8	15.4
k or K −80 °C	1.4–1.6 × 10^8	240	6.5 × 10^5

[a] ΔH, kJ mol^{-1}. [b] ΔS, J K^{-1} mol^{-1}. [c] In MeTHF, this work. [d] In THF, determined through flash-and-trap method.[13] Values for [(TMPA)−Cu] in MeTHF have been found to be the same as in THF within experimental errors.

the same thermodynamic parameters within the experimental errors and are consistent with values found in a previous report by Roth and co-workers (Table S1 and Figures S2 and S5 in SI). Furthermore, equilibrium constants found in this work follow a trend with solvent dielectric constant (ε) that was previously established.[12a] The equilibrium constant should favor the superoxide adduct as ε increases because of the stabilization of the charge separation present in **1**. In fact, the equilibrium constant for the formation of **1** (K_{O_2}) determined here at −60 °C fits well into a linear correlation together with the previously determined K_{O_2} values in DMF (3030 and 4340)[12a] and in chlorobenzene (216)[12] at −60 °C as a function of ε (see SI).

A comparison of activation and thermodynamic parameters determined in this study with those previously reported for the $[(TMPA)Cu^{II}(O_2)]^+$ adduct in MeTHF using $[(TMPA)Cu^I(CO)]^+$ and the "flash-and-trap" method are also given in Table 1 (see Chart 1 for structure of ligands). This complex has

Chart 1

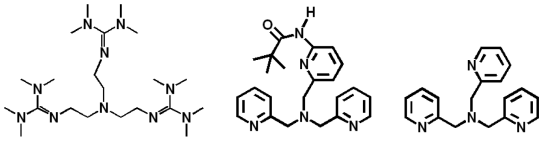

been very well studied and it is the 'parent' ligand of PV-TMPA.[1a,13,14] The "flash-and-trap" experiments, previously employed for $[(L)Cu^I(CO)]^+$ (L = ligand) compounds, allowed characterization of O_2 binding to copper(I) after CO photorelease through competitive coordination of CO and O_2.[13,14] The kinetic data obtained through the direct O_2

dx.doi.org/10.1021/ja4115314 | J. Am. Chem. Soc. 2014, 136, 1260−1263

photoejection method described here are more straightforward to analyze compared to that of the "flash-and-trap" method where the competitive binding of CO needs to be taken into account. Furthermore, in fast time-scale studies of heme–copper oxidases, it has been shown that the presence of CO and starting with a metal–CO adduct may interfere or alter the mechanism or rate of O_2 binding.[15] The activation parameters found for the compounds studied here are quite similar to those previously determined by the flash-and-trap method, providing strong evidence for the reliability of the new method we have employed here to study the reactivity of mononuclear copper compounds with O_2.

TMG_3tren, PV-TMPA, and TMPA offer an analogous coordination sphere to the copper ion, all being tetradentate chelating ligands to study and compare their copper(I) complex O_2-binding properties under the same experimental conditions (solvent, temperature, etc.). The activation enthalpy found for the binding of O_2 to **3** and **4** falls within the same range (~10 kJ mol^{-1}). On the basis of the crystal structure of the starting compound $[(PV\text{-}TMPA)Cu^{I}]^{+}$,[11] the coordination within **4** most likely also includes an interaction between the copper(I) ion and the O atom of the pivalamido group. As a consequence, one would expect a higher activation enthalpy for the reaction between O_2 and **4** compared with that between O_2 and **3** as the Cu(I)–O interaction needs to be "disrupted" by O_2 coordination to **4** but not for **3**. Since the $\Delta H^{\ddagger}$ values for the binding of O_2 to **3** and **4**, instead, fall into the same range, this suggests a quite weak interaction for the Cu^{I}–$O_{(carbonyl)}$ coordination in **4**. Instead, the activation entropy estimated for the reaction involving O_2 coordination to **3** and to **4** is smaller for the latter. This suggests a mechanism where O_2 coordination to **4** leads to a "highly ordered" transition state where both O_2 and the pivalamido O atom are interacting with the copper center; for O_2 reacting with **3**, there is, of course, no pivalamido group present.

The activation enthalpy and entropy for O_2 coordination to $[(TMPA)Cu^{I}]^{+}$ previously determined (Table 1) are smaller and less negative, respectively, compared with those found for **3** and **4**. This can be interpreted on the basis of a stronger Cu–O_2 interaction in the transition state for $[(TMPA)Cu^{I}]^{+}$ compared to that for **3** and **4** due to an "easier" spatial approach of O_2 to the copper(I) in $[(TMPA)Cu^{I}]^{+}$. In fact, the presence of guanidino groups which extend out away from the copper and its ligands in **3**, and of the Cu^{I}–$O_{(carbonyl)}$ coordination, in **4**, would support this hypothesis. The less negative activation entropy found for the coordination of O_2 to $[(TMPA)Cu^{I}]^{+}$ could reflect a smaller molecular reorganization occurring upon O_2 binding to $[(TMPA)Cu^{I}]^{+}$ due to the absence of guanidino groups or specific Cu(I)–O interactions in $[(TMPA)Cu^{I}]^{+}$ compared with **3** and **4**. Similar arguments can be used to interpret the difference between the activation enthalpy found for the O_2 dissociation from $[(TMPA)\text{-}Cu^{II}(O_2)]^{+}$ with the "flash-and-trap" method and those found here for **1** and **2**, although the large activation entropy found for O_2 dissociation from $[(TMPA)Cu^{II}(O_2)]^{+}$ seems unclear.

TD-DFT calculations are in line with the previously assigned electronic ground state for **1**.[10,12,16] In this rather peculiar electronic structure, the central copper ion is in a d^9 configuration and coordinated to a superoxide ligand. The singly occupied MOs are of copper $3d_{z^2}$ and $O_2^{\bullet-}$–π^*_v character. The orthogonality of these two orbitals leads to a S = 1 ground state multiplicity in which the spin in both SOMOs are aligned parallel (see SI). In a spin-unrestricted description, the highest occupied spin-down orbital has mainly oxygen π^*_σ character, and it is bonding with respect to the Cu^{II}–superoxide Cu–O bond. The lowest unoccupied orbitals in the spin-down manifold are the empty partner orbitals of the two SOMOs. Importantly, the unoccupied $3d_{z^2}$ orbital is strongly σ-antibonding with respect to the Cu–O bond. Excitation from the bonding π^*_σ -based orbital to the antibonding d_{z^2} orbital corresponds to a ligand-to-metal charge transfer (LMCT) excitation that formally leads to a Cu(I)–$^3O_2$ electronic configuration. Importantly, this excitation leads to a dramatic weakening of the Cu–O bond to the point that the excited state becomes dissociative (Figure 2).

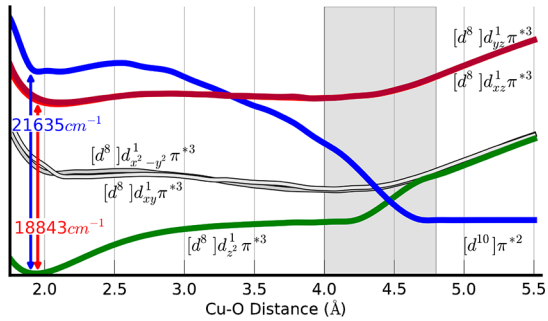

Figure 2. TD-DFT calculated excited state potential energy surfaces (PESs) as a function of copper–oxygen bond distance.

As is evident from Figure 3, there is an avoided crossing of the d_{z^2} and π^* orbitals upon elongation of the Cu–O bond,

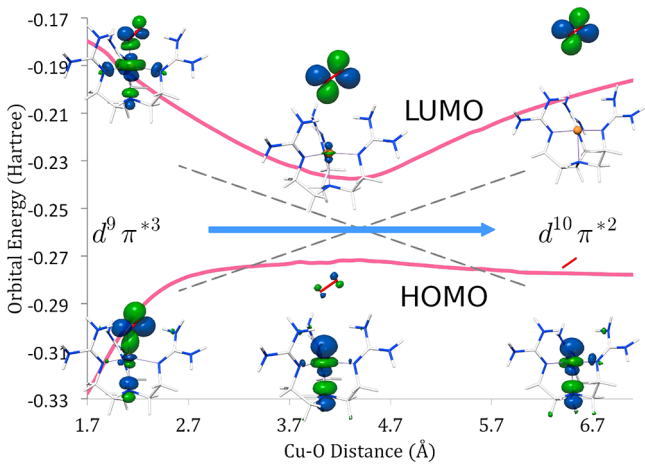

Figure 3. TD-DFT calculated energy and shape of the β-HOMO and β-LUMO orbitals as a function of copper–oxygen bond distance.

resulting in a change from a triplet Cu(II) superoxide ground state $[d^8]$–$d_{z^2}{}^1\pi^{*3}$ to a triplet Cu(I)–$^3O_2$ ($d^{10}\pi^{*2}$) state at the dissociation limit. The triplet ground-state potential energy surface of **1** (Figure 2, green line) shows a minimum at a Cu–O distance of about 1.9 Å. The calculated excited state energy at the same Cu–O bond distance was 18,843 cm^{-1} (530 nm) for the d–d and 21,635 cm^{-1} (462 nm) for the LMCT transition, consistent with the experimentally observed electronic transitions for these states. Moreover, the character of both excited states at a Cu–O bond distance of 1.9 Å is dissociative (Figure 2). The LMCT excited state (blue line) crosses the ground state at a Cu–O distance of about 4.5 Å. As the dissociative LMCT state crosses the d–d excited states

dx.doi.org/10.1021/ja4115314 | J. Am. Chem. Soc. 2014, 136, 1260–1263

(shown in red) there is an opportunity for the system to cross from one of the d−d excited surfaces to the dissociative LMCT surface. Hence, there can also be O_2 dissociation following d−d excitation, provided that these states live long enough to reach the crossing regime. The exact crossing probability will depend on many details, the discussion of which is outside the scope of this work. Given the finite probability for surface hopping, much lower quantum yields are theoretically predicted for d−d excitations. This is in agreement with the observations for O_2 photorelease observed experimentally following excitation of **1** with either red (ϕ_{683} = 0.035) or blue light (ϕ_{436} = 0.29). The theoretical results are also consistent with the activation enthalpy for the O_2 dissociation from **1** observed experimentally ($\Delta H^{\ddagger}_{exp}$ = 45 kJ mol^{-1} vs $\Delta H^{\ddagger}_{comput}$ = 67 kJ mol^{-1}).

Finally, the crossing between the ground state (green) and LMCT (blue) surfaces explains the fact that an association barrier is observed for O_2-rebinding. The calculated barrier from TD-DFT (∼24 kJ mol^{-1}) is close but slightly overestimates the experimentally measured barrier (∼10 kJ mol^{-1}).

Summarizing, we report here the first example of a photodissociation of molecular oxygen from cupric−superoxide complexes, thus also representing a new approach to study the kinetics and the thermodynamics of the formation of 1:1 ligand copper(I)/O_2 compounds. Copper−oxygen bond breaking is induced in $[(TMG_3tren)Cu^{II}(O_2)]^+$ and $[(PV\text{-}TMPA)\text{-}Cu^{II}(O_2)]^+$ through laser excitation either into the LMCT band, using 436 nm light, or into the d−d electronic transition, using 683 nm light. Interestingly, the quantum yield for O_2 release was wavelength dependent. TD-DFT studies elucidated the O_2 photorelease event occurring upon irradiation with red light on the basis of (a) population of a molecular orbital ($3d_{z^2}$) that has strong σ-antibonding character along the Cu−O bond and (b) energy surface crossing between the d−d and the LMCT excited states to lead to O_2 release. Such findings add new insights into the observed wavelength dependent Cu/O_2 photochemistry which differs markedly from that observed with hemes, where for example, the O_2 adduct of myoglobin releases O_2 with a quantum yield of 0.3 following Soret (λ_{exc} = 488 nm) or Q (λ_{exc} = 580 nm) band excitation.[9] Formation and decay of $[(TMG_3tren)Cu^{I}]^+$ and $[(PV\text{-}TMPA)Cu^{I}]^+$ formed in situ have been observed, and both activation and thermodynamic parameters for the Cu/O_2 reactions have been determined. Additional experimental studies are on their way to further characterize the excited states involved in the copper−oxygen bond-breaking process using ultrafast laser spectroscopy.

■ ASSOCIATED CONTENT

Supporting Information

Experimental procedures, spectra, explanations, DFT calculations and supporting diagrams. This material is available free of charge via the Internet at http://pubs.acs.org.

■ AUTHOR INFORMATION

Corresponding Author

karlin@jhu.edu

Notes

The authors declare no competing financial interest.

■ ACKNOWLEDGMENTS

K.D.K. acknowledges financial support of this research from the National Institutes of Health, R01 GM28962. G.J.M. is grateful for research support from the National Science Foundation, CHE-1213357. F.N. acknowledges research support from the Max Planck Society.

■ REFERENCES

(1) (a) Fukuzumi, S.; Karlin, K. D. *Coord. Chem. Rev.* **2013**, *257*, 187. (b) Himes, R. A.; Karlin, K. D. *Curr. Opin. Chem. Biol.* **2009**, *13*, 119. (c) Solomon, E. I.; Ginsbach, J. W.; Heppner, D. E.; Kieber-Emmons, M. T.; Kjaergaard, C. H.; Smeets, P. J.; Tian, L.; Woertink, J. S. *Faraday Discuss.* **2011**, *148*, 11. (d) Allen, S. E.; Walvoord, R. R.; Padilla-Salinas, R.; Kozlowski, M. C. *Chem. Rev.* **2013**, *113*, 6234.

(2) Maiti, D.; Lee, D. H.; Gaoutchenova, K.; Wurtele, C.; Holthausen, M. C.; Sarjeant, A. A.; Sundermeyer, J.; Schindler, S.; Karlin, K. D. *Angew. Chem., Int. Ed.* **2008**, *47*, 82.

(3) Maiti, D.; Narducci Sarjeant, A. A.; Karlin, K. D. *Inorg. Chem.* **2008**, *47*, 8736.

(4) (a) Comba, P.; Knoppe, S.; Martin, B.; Rajaraman, G.; Rolli, C.; Shapiro, B.; Stork, T. *Chemistry* **2008**, *14*, 344. (b) Decker, A.; Solomon, E. I. *Curr. Opin. Chem. Biol.* **2005**, *9*, 152. (c) Yoshizawa, K.; Kihara, N.; Kamachi, T.; Shiota, Y. *Inorg. Chem.* **2006**, *45*, 3034. (d) Crespo, A.; Marti, M. A.; Roitberg, A. E.; Amzel, L. M.; Estrin, D. A. *J. Am. Chem. Soc.* **2006**, *128*, 12817. (e) Huber, S. M.; Ertem, M. Z.; Aquilante, F.; Gagliardi, L.; Tolman, W. B.; Cramer, C. J. *Chemistry* **2009**, *15*, 4886.

(5) (a) Blackburn, N. J.; Rhames, F. C.; Ralle, M.; Jaron, S. *J. Biol. Inorg. Chem.* **2000**, *5*, 341. (b) Prigge, S. T.; Mains, R. E.; Eipper, B. A.; Amzel, L. M. *Cell. Mol. Life Sci.* **2000**, *57*, 1236.

(6) Stewart, L. C.; Klinman, J. P. *Annu. Rev. Biochem.* **1988**, *57*, 551.

(7) (a) Evans, J. P.; Ahn, K.; Klinman, J. P. *J. Biol. Chem.* **2003**, *278*, 49691. (b) Klinman, J. P. *Chem Rev* **1996**, *96*, 2541. (c) Klinman, J. P. *J. Biol. Chem.* **2006**, *281*, 3013. (d) Bauman, A. T.; Yukl, E. T.; Alkevich, K.; McCormack, A. L.; Blackburn, N. J. *J. Biol. Chem.* **2006**, *281*, 4190.

(8) (a) Chen, P.; Solomon, E. I. *J. Am. Chem. Soc.* **2004**, *126*, 4991. (b) Cramer, C. J.; Tolman, W. B. *Acc. Chem. Res.* **2007**, *40*, 601. (c) Chen, P.; Bell, J.; Eipper, B. A.; Solomon, E. I. *Biochemistry* **2004**, *43*, 5735.

(9) Ye, X.; Demidov, A.; Champion, P. M. *J. Am. Chem. Soc.* **2002**, *124*, 5914.

(10) (a) Schatz, M.; Raab, V.; Foxon, S. P.; Brehm, G.; Schneider, S.; Reiher, M.; Holthausen, M. C.; Sundermeyer, J.; Schindler, S. *Angew. Chem., Int. Ed.* **2004**, *43*, 4360−4363. (b) Würtele, C.; Gaoutchenova, E.; Harms, K.; Holthausen, M. C.; Sundermeyer, J.; Schindler, S. *Angew. Chem., Int. Ed.* **2006**, *45*, 3867−3869. (c) Woertink, J. S.; Tian, L.; Maiti, D.; Lucas, H. R.; Himes, R. A.; Karlin, K. D.; Neese, F.; Wurtele, C.; Holthausen, M. C.; Bill, E.; Sundermeyer, J.; Schindler, S.; Solomon, E. I. *Inorg. Chem.* **2010**, *49*, 9450.

(11) Peterson, R. L.; Himes, R. A.; Kotani, H.; Suenobu, T.; Tian, L.; Siegler, M. A.; Solomon, E. I.; Fukuzumi, S.; Karlin, K. D. *J. Am. Chem. Soc.* **2011**, *133*, 1702.

(12) (a) Lanci, M. P.; Smirnov, V. V.; Cramer, C. J.; Gauchenova, E. V.; Sundermeyer, J.; Roth, J. P. *J. Am. Chem. Soc.* **2007**, *129*, 14697. (b) Lide, D. R. *CRC Handbook of Chemistry and Physics, 74th ed.*, CRC Press: Boca Raton, 1993.

(13) Fry, H. C.; Scaltrito, D. V.; Karlin, K. D.; Meyer, G. J. *J. Am. Chem. Soc.* **2003**, *125*, 11866.

(14) Lucas, H. R.; Meyer, G. J.; Karlin, K. D. *J. Am. Chem. Soc.* **2010**, *132*, 12927.

(15) (a) Elinarsdóttir, Ó.; Funatogawa, C.; Soulimane, T.; Szundi, I. *Biochim. Biophys. Acta* **2012**, *1817*, 672. (b) Szundi, I.; Funatogawa, C.; Fee, J. A.; Soulimane, T.; Elinarsdóttir, Ó. *Proc. Natl. Acad. Sci. U.S.A.* **2010**, *107*, 21010.

(16) (a) Poater, A.; Cavallo, L. *Inorg Chem* **2009**, *48*, 4062. (b) Zapata-Rivera, J.; Caballol, R.; Calzado, C. J. *J. Comput. Chem.* **2011**, *32*, 1144.